

Fig. 2 Main bars for HSCT wing optimal design; flexible fuselage.

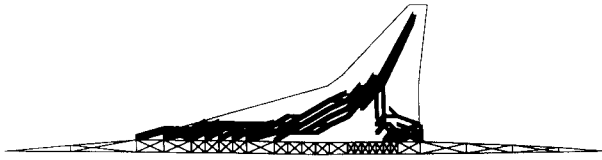


Fig. 3 Main bars for HSCT wing optimal design; flexible fuselage; refined mesh.

Effect of Mesh Density

Our next step was to investigate the effect of mesh density for the HSCT model with flexible fuselage. The mesh used in the previous step was refined. The refined ground structure consists of 436 nodes and 3015 bars. 180 nodes and 337 bars of this ground structure were used to define the fuselage. The weights of the fuselage and of the wing and the boundary conditions were the same as for the less refined mesh. The same total load was distributed now at 430 nodes (again, all nodal points except for the six fixed ones).

The optimal structure for this case has a relative compliance of 77.39% compared to the ground structure (i.e., a factor of 1.29 increase in stiffness).

The main bars, accounting for 90.6% of V_w , are shown in Fig. 3. Comparison with the results obtained for the coarser mesh shows that the location of the main bars is almost the same.

Conclusions

The problem of designing efficient wing internal structure for the HSCT was considered. The ground structure approach with an algorithm due to Ben-Tal and Bendsøe¹ was used to solve this problem. The main simplifying assumptions were modeling the aircraft internal structure as a truss and using compliance as a single criterion for the design. In spite of these simplifications we hope that the results obtained provide an indication of the kind of internal structure required for the HSCT wing.

Based on the results of the work described in this Note we may conclude the following:

- 1) Compliance minimization based on ground structure approach is feasible for three-dimensional structures, but requires reduced connectivity to reduce the number of bars.
- 2) Fuselage flexibility has a large effect on topology, especially in the inboard wing area.
- 3) Refining the mesh and the load distribution did not lead to substantial changes in topology.

Acknowledgment

This work was supported by NASA Grant NAG1-168.

References

- ¹Ben-Tal, A., and Bendsøe, M. P., "A New Method for Optimal Truss Topology Design," *SIAM Journal on Optimization*, Vol. 3, No. 2, 1993, pp. 322-358.
- ²Balabanov, V. O., and Haftka, R. T., "Topology Optimization of Transport Wing Internal Structure," AIAA Paper 94-4414, Sept. 1994.
- ³Hutchison, M. G., Huang, X., Mason, W. H., Haftka, R. T., and Grossman, B., "Variable-Complexity Aerodynamic-Structural Design of a High-Speed Civil Transport Wing," AIAA Paper 92-4695, Sept. 1992.

Analytic V Speeds from Linearized Propeller Polar

John T. Lowry*

Flight Physics, Billings, Montana 59104-0919

Introduction

THE primary fixed-pitch, propeller-driven, normally aspirated aircraft flight performance V speeds (best angle of climb speed V_x , best rate of climb speed V_y , maximum level speed V_m) are given by simple analytic expressions when ordinary power-available/power-required (P_{av}/P_{rc}) analysis is combined with the assumption¹ of linearity of the propeller polar: $C_T/J^2 = mC_p/J^2 + b$. Constants m and b can be obtained from propeller charts or by flight tests. (Because we often know more about power than thrust, we have reversed, relative to Von Mises's usage, the independent and dependent variables.) We also require an expression for the drop in engine torque M with relative atmospheric density σ , from its standard mean sea level (MSL) value M_0 ; we use essentially that of Gagg and Farrar²: $M(\sigma) = \phi(\sigma)M_0 = M_0(\sigma - C)/(1 - C)$. C is in the range $[0.11, 0.15]$ and can be obtained from the usual engine chart or approximated (Gagg and Farrar's value was 0.117) as 0.12. We focus on torque, rather than on brake power, because torque is nearly constant at constant throttle position (or manifold absolute pressure) and altitude. A few pieces of operating handbook data on the aircraft are needed, as is a drag polar for the configuration under consideration. The simplicity of the resulting expressions may be useful in preliminary flight testing and as a pedagogical tool for students of aircraft performance.

These ideas share motivation and basic features with Ref. 1, Chapter XV. Major differences between our treatments are as follows:

- 1) His dimensionless variables are less transparent than our manifestly engineering ones.
- 2) He uses a representative propeller blade element in place of our focus on the linearized polar parameters.
- 3) He requires several arguments concerning small quantities or neglected terms of second order while we need not do so.
- 4) Some of his results are series expansions while ours are all in closed form.

The straightforwardness of the development discussed next allows it to not only derive simple formulas for the various full-throttle V speeds (as functions of gross aircraft weight W and atmospheric density ρ), but also such results as 1) the independence of V_x , in calibrated terms, of density altitude and 2) formulas connecting V_x , V_y , and V_m (all at the same W and ρ). The necessity of that latter result can be argued for by simply counting unknown parameters and given relations.

With a few additional assumptions, and recording of revolutions per minute data, this work can be extended to partial-throttle performance, to takeoff and landing performance, and to constant-speed propeller operation. We won't make those extensions here. Its small number of assumptions gives this treatment a boundedness that may keep the student from being sidetracked. Armed with an ordinary spreadsheet program he or she can easily generate concrete graphs or tables showing a given airplane's steady flight characteristics.

Received Jan. 28, 1995; revision received July 1, 1995; accepted for publication July 1, 1995. Copyright © 1995 by J. T. Lowry. Published by the American Institute of Aeronautics and Astronautics, Inc., with permission.

*Owner, 724 Alderson Avenue, P.O. Box 20919.

Required Data

The data needed for concrete analysis of the airplane's V -speed flight performance, partitioned into logical groups, consists of only the following:

- 1) Atmosphere: Density ρ (or relative density $\sigma = \rho/\rho_0$).
- 2) Airframe: Gross weight W , reference wing area S , wing aspect ratio $A (=B^2/S, B = \text{wingspan})$, parasite drag coefficient C_{D0} , and airplane efficiency factor e . (In fact, W and A could be replaced by span loading W/B .)
- 3) Engine: Rated full-throttle MSL torque $M_0 = P_0/2\pi n_0$ (P_0 rated power, n_0 rated propeller rps), and the aforementioned torque dropoff parameter C , the fractional internal frictional losses independent of altitude.
- 4) Propeller: Slope of the propeller polar m , intercept of the propeller polar b , and propeller diameter d .

There are eleven numbers in all. For a given flaps/gear configuration, only ρ and W are variable; of the nine other parameters, S , A , d , and M_0 are easily obtained from the Pilots Operating Handbook or Approved Flight Manual. C can be obtained by averaging on the right-hand side of the engine chart or assigned value 0.12. We still need the more problematic values of C_{D0} , e , m , and b . Glide tests can give the first two. Propeller charts or, more likely, climb and full-speed tests at given W and ρ (to be detailed) can give the last two.

With the 11 numerical players identified, we turn our attention to the connections between the three V speeds and P_{av}/P_{re} analysis. V_m , V_y , and V_x are simply related to the excess power $f = P_{av} - P_{re}$ = power available - power required = $TV - DV$. T is thrust force, D is drag force, and V is true airspeed. In particular, V_m is the (upper) solution of $f = 0$; V_y is the solution of $f' = 0$ (here, ' denotes derivatives with respect to V); and V_x is the solution of $(f/V)' = 0$.

Plan and Details

We find expressions for the three V speeds in terms of our 11 numbers. It turns out that four combinations of parameters (we'll call them E , F , G , and H) will do the job. And, in fact, $K = (F - G)$, along with E and H , will do it. Once glide tests determine C_{D0} and e , we shall have even more than we need, three conditions (in E , K , and H) to determine two parameters m and b . Now for the details.

On the power-available side, use the definitions of advance ratio ($J = V/nd$) and propeller thrust coefficient C_T :

$$P_{av} = TV = \rho n^2 d^4 C_T (J) V \quad (1)$$

We also need the definitions of shaft power P and of the propeller power coefficient:

$$C_p = P/\rho n^3 d^5 \quad (2)$$

Using these definitions and assumptions with the linearized propeller polar and the definition of $\phi(\sigma)$ given previously, we find

$$P_{av} = EV + FV^3 \quad (3)$$

where

$$E = \frac{m\phi(\sigma)P_0}{n_0 d} \quad (4)$$

$$F = \rho d^2 b \quad (5)$$

On the power-required side, we use the usual quadratic drag polar

$$D = \frac{1}{2}\rho V^2 S \left[C_{D0} + \left(\frac{C_L^2}{\pi e A} \right) \right] \quad (6)$$

and (for these small flight angles) the essential equality of weight W and lift L

$$W = L = \frac{1}{2}\rho V^2 S C_L \quad (7)$$

to get

$$P_{re} = GV^3 + H/V \quad (8)$$

where

$$G = \frac{1}{2}\rho S C_{D0} \quad (9)$$

$$H = 2W^2/\rho S \pi e A \quad (10)$$

In terms of our composite parameters E , F , G , and H

$$f \equiv P_{av} - P_{re} = EV + (F - G)V^3 - H/V \quad (11)$$

Recall $K = F - G$. Now consider each of the V speeds separately.

Maximum level flight speed V_m is given by (the larger solution of) $f = 0$. Using the form just given, multiplying by V , letting $V^2 = Z$, and solving (choosing the proper sign, using $K < 0$)

$$V_m = \sqrt{(-E - \sqrt{E^2 + 4KH})/2K} \quad (12)$$

Speed for the best rate of climb V_y is given by $f' = 0$ or

$$f' = E + 3KV^2 + H/V^2 = 0 \quad (13)$$

Multiply by V^2 , again let $V^2 = Z$, and solve to find

$$V_y = \sqrt{(-E - \sqrt{E^2 - 12KH})/6K} \quad (14)$$

Speed for best angle of climb V_x is given by $(f/V)' = 0$ or

$$(f/V)' = 2KV + 2H/V^3 = 0 \quad (15)$$

Multiply by $V^3/2$ and take roots to get

$$V_x = (-H/K)^{1/4} \quad (16)$$

Equation (16), with a glance at the density dependence of H/K , shows that calibrated airspeed V_x is independent of air density. In gliding flight, when P_{av} is zero ($E = F = 0$), V_x becomes speed for best glide V_{bg} . Hence, calibrated V_{bg} is also independent of density altitude; it does, of course, depend on gross weight. Under these power-off conditions there is no physical solution for V_m . But it's satisfying that V_y simply becomes the speed for minimum descent V_{md} , and, as is well known, is $(\frac{1}{3})^{1/4} V_{bg}$.

For a given airplane configuration there are only two variable combinations required, E/K and H/K . This means any one of our three V speeds should be obtainable from knowledge of the other two. Pursuing this train of thought, a little algebra gives

$$V_x = \left(\frac{3V_y^2 - V_m^2}{V_m^{-2} + V_y^{-2}} \right)^{1/4} \quad (17)$$

Flight Test Procedures

Now it is time for flight tests to determine the required parameters for a given airplane in a given configuration. Here is one possible scenario:

1) Do glide tests (knowing the best glide angle, and the speed for it, for given W and σ is sufficient). This gives C_{D0} and e , which in turn gives G and H . A reviewer accurately pointed out that getting drag polar parameters from glide tests is a tricky business; a windmilling propeller produces extra drag, stable air is required, and nonstandard temperature lapse rates must be accounted for. It would be best to use the zero-thrust apparatus and careful techniques pioneered by Norris and Bauer.³

2) Do best angle of climb tests for V_x . Since we know H , this gives us $K = (F - G)$. Since we know G , this gives us F , which gives us the propeller polar intercept b . The required inversion is

$$b = \frac{SC_{D0}}{2d^2} - \frac{2W^2}{\rho^2 d^2 S \pi e A V_x^4} \quad (18)$$

For an intuitively correct power drop factor, b will be negative.

3) Do either maximum level flight speed tests for V_m or best rate of climb tests for V_y . Since we have H and K , either will give us E , which will give us propeller polar slope m . Using an experimental V_m ,

$$m = \frac{2n_0 d W^2}{\phi(\sigma) P_0 \rho S \pi e A} \left(\frac{1}{V_m^2} + \frac{V_m^2}{V_x^4} \right) \quad (19)$$

while using an experimental V_y ,

$$m = \frac{2n_0 d W^2}{\phi(\sigma) P_0 \rho S \pi e A} \left(\frac{3V_y^2}{V_x^4} - \frac{1}{V_y^2} \right) \quad (20)$$

Once these three tests (plus POH information) complete our knowledge of the 11 numbers, we can find any or all of the three V speeds (or P_{av} , P_{re} , thrust, drag, or anything that depends on any of these) for any desired values of gross weight and atmospheric density (or density altitude).

Conclusions

This analysis allows realistic flight performance prediction without propeller charts; those are often hard to get and, even if available, need to be corrected for fuselage profile. The technique is remarkably fertile, needing little time to make graphs showing density altitude and weight dependencies of each of V_m , V_y , and V_x ; P_{av} and P_{re} curves; rates and angles of climb for various speeds, weights, and altitudes; the same for sink rates; the speed dependence of parasite, induced and total drag force; and absolute ceilings, and speed there, for a given weight.

References

- ¹Von Mises, R., *Theory of Flight*, Dover, New York, 1959, pp. 308, 309, 398, 423, 424.
- ²Gagg, R. F., and Farrar, E. V., "Altitude Performance of Aircraft Engines Equipped with Gear-Driven Superchargers," *Society of Automotive Engineers Transactions*, Vol. 29, 1934, pp. 217-223.
- ³Norris, J., and Bauer, A. B., "Zero-Thrust Glide Testing for Drag and Propulsive Efficiency of Propeller Aircraft," *Journal of Aircraft*, Vol. 30, No. 4, 1993, pp. 505-511.

Flight Testing a General Aviation Head-Up Display

M. W. Anderson*

Federal Aviation Administration,
Des Plaines, Illinois 60018
and

D. D. French,† R. L. Newman,‡ and M. R. Phillips§
Flight Visions, Inc., Sugar Grove, Illinois 60554

Introduction

THE head-up display (HUD) was originally developed for military aircraft from reflecting optical sights. The HUD places flight and navigation data in the pilot's forward field of view (FOV). This data symbology is presented as a collimated image that appears to be floating at infinity. A semitransparent mirror (the combiner) allows the pilot to view the symbols simultaneously with the real world.

A typical HUD presents the information from the basic T instruments: airspeed, altitude, pitch and roll attitude, and heading. In addition, appropriate course (and glide slope) deviation data can be selected for display. Distance measuring equipment (DME), flight director, radar altitude, and marker beacon passage can be shown if available.

The HUD can also be used to display other information, such as master warning/caution information, an electronic checklist, and a stopwatch timer.

Aircraft Constraints

The FV-2000 HUD was developed as a low-cost display for retrofit into executive and corporate aircraft. Several constraints became apparent at the outset. The space available in the candidate airframes limited the combiner size. The resultant FOV is rather small, approximately 9 deg.

To minimize cost, the FV-2000 differs from most military and transport HUDs in that it uses conventional aircraft gyros rather than an inertial platform for attitude information. This created a potential problem since the aircraft gyros are less accurate than inertial platforms.

The small FOV and the potential difficulty in providing accurate registration led to a decision not to insist on conformity with the external visual scene. To minimize any subjective discomfort, the HUD symbology is compressed relative to the real world. This has the added benefit of enhancing pilot spatial orientation. The remaining design issues dealt with cockpit integration: always a problem when retrofitting a digital display into an existing analog cockpit.

HUD Criteria

There are no criteria for head-up displays in the civil community. In fact, at the time, there were no agreed upon criteria for HUDs in any community, civil or military. Criteria had to be developed for the King Air installation.

Generally, existing guidelines were used to the extent possible. Advisory Circular 25-11 (Ref. 1) was used for many of

Received May 1, 1995; revision received Aug. 1, 1995; accepted for publication Aug. 8, 1995. Copyright © 1995 by the American Institute of Aeronautics and Astronautics, Inc. All rights reserved.

*Flight Test Pilot, Aircraft Certification Office, 2300 East Devon Avenue, Member AIAA.

†Pilot, P.O. Box 250.

‡Project Pilot, P.O. Box 250; currently DER Flight Test Pilot, Crew Systems, P.O. Box 963, San Marcos, TX 78667. Associate Fellow AIAA.

§Vice President, P.O. Box 250.